Associating Monthly Hail Occurrence and Large Scale Environment for the Continental United States

JOHN T. ALLEN*

International Research Institute for Climate and Society, Columbia University, Palisades, New York

MICHAEL K. TIPPETT

Department of Applied Physics and Applied Mathematics, Columbia University, New York, New York

Center of Excellence for Climate Change Research, Department of Meteorology, King Abdulaziz University, Jeddah, Saudi Arabia

ADAM H. SOBEL

Department of Applied Physics and Applied Mathematics, Department of Earth and Environmental Sciences, Columbia University, New York, New York

*Corresponding author address: J. T. Allen, International Research Institute for Climate and Society, The Earth Institute of Columbia University, Lamont Campus 61 Route 9W, Palisades New York 10964, USA.

E-mail: JohnTerrAllen@gmail.com

ABSTRACT

A new index relating large hail occurrence to environmental parameters has been developed. Hail events are defined as the total number of three-hourly periods in a month that experience one or more instance of hail larger than one inch. The index is derived using Poisson regression between hail events and monthly mean variables describing the large scale environment from the North American Regional Reanalysis (NARR) over the period 1979-2012. The index depends on four parameters; convective precipitation, convective available potential energy, storm relative helicity and the mean specific humidity between the surface and 90hPa. The new index differs in its choice of parameters and their weighting from existing indices for the occurrence of either hail or tornadoes. The index performs well simulating the monthly climatology of CONUS and regional total occurrence of large hail. The spatial distribution of the index also favorably represents the hail event climatology. However, in the index, the westward shift of maximum hail frequency during the summer months is delayed relative to observations. Additionally, for the area just east of the Rocky mountains, the index has a lower frequency of hail compared to observations. Despite these limitations, annual index variations are realistic when compared to de-trended observations of hail frequency. Little trend is seen in the index compared to the large increases in hail reports over the three decades. The development of this hail index allows for future exploration into climate scale linkages, the potential for seasonal forecasting and analysis of hail frequency under climatic change.

1. Introduction

Hail causes intense local damage. While not completely destroying structures, hail affects larger areas than tornadoes do, and resulted in annual losses approaching 1 billion US dollars per year in the United States (US) in the early 2000s (Changnon 1999, 2008). While the largest hailstones typically receive the most attention, hail greater than one inch can still cause significant damage to agricultural resources, vehicles and buildings.

The majority of hailstones equal to or larger than one inch (hereafter large hailstones) are associated with organized thunderstorms (Kelly et al. 1985), and nearly all instances of hail in excess of two inches in diameter (hereafter giant hail) are associated with supercell thunderstorms, though these stones may only occupy a small part of the hail from a storm (Changnon et al. 2009).

The US National Climatic Data Center's Storm Data observational hail record is the most comprehensive publicly available data set. However, it has a number of deficiencies (Schaefer and Edwards 1999; Doswell et al. 2005; Doswell 2007). For example, only the maximum hail size is reported, and that value may be quantized or distorted by association to reference objects (e.g., golfballs) rather than representing a direct measurement. Recent high-resolution hail observations from field campaigns (e.g Ortega et al. 2009; Blair et al. 2014) suggest that larger hail sizes are more common than would be expected from Storm Data. Another characteristic of the Storm Data hail is the spatially variable positive trends found in reports of giant hail, with greater increases over the southeast of the United States (Schaefer et al. 2004). These trends skew heavily towards areas of higher population density, and where National Weather Service forecast offices actively seek out hail reports to contribute to the warning verification process (Hales Jr 1993; Wyatt and Witt 1997; Davis and LaDue 2004; Schaefer et al. 2004; Trapp et al. 2006; Cintineo et al. 2012). These factors make analysis of trends in hail occurrence, and understanding the spatial and seasonal characteristics of hail from existing observational data difficult.

An alternative technique used to investigate variability and trends in hail occurrence is to con-

sider the environments that are favorable to the development of hail (Brooks et al. 2003; Brooks 2009). Hail occurrence has previously been related to the thermodynamic potential of the severe thunderstorm environment (Stumpf et al. 2004; Groenemeijer and Van Delden 2007; Grams et al. 2012; Thompson et al. 2012), particularly the steepness of mid-level lapse rates, suspension of ice nuclei in the optimum hail growth region, as well as moisture availability. While thermodynamic sources of energy are essential to promote the strong updrafts that support hail, another important contribution comes from shear enhancement of the vertical pressure gradient in strengthening updrafts (Edwards and Thompson 1998; Doswell III and Markowski 2004; Jewell and Brimelow 2009; Grams et al. 2012; Manzato 2012). This interaction is quantified, for example, in the operationally applied Significant Hail Parameter (SHIP[1]), which is used to identify the likelihood of conditions favorable to the development of giant hail. SHIP is a function of convective available potential energy (CAPE), the mixing ratio of a parcel, environmental mid-level lapse rate, 500hPa temperature and 0-6km vertical wind shear (S06). In comparison, the significant severe categorization of Brooks et al. (2003) attempts to capture giant hail as well as damaging winds and strong tornadoes using the product of CAPE and S06.

The primary difference between the significant severe parameter and SHIP is that the latter has a greater dependence on the thermodynamics of the profile, particularly the mid-level lapse rate, and moisture available. However, other complex interactions on the microphysical scale, moisture loading, as well as the structure of the vertical temperature profile can influence the potential for large hail, meaning that climatological indices for other severe phenomena (tornadoes; Tippett et al. 2012, 2014, significant severe thunderstorms; Brooks et al. 2003; Gensini and Ashley 2011) may not be appropriate for estimating hail occurrence. As illustrated by Brooks (2013), the parameters of importance for different modes of severe weather phenomena vary in terms of the thermodynamic and kinematic balance, suggesting greater strength in ingredient/parameter-based

[1]Details of the formula for the significant hail parameter can be found at `http://www.spc.noaa.gov/exper/mesoanalysis/help/help_sigh.html`

relationship may be achieved by stratifying severe environment indices into tornado, hail and wind categorizations.

The total number of tornado and hail (in excess of one inch) reports per year over the continental United States (CONUS) for the period 1979-2012 is shown in Figure 1. Relative to the tornado climatology, hail is found further to the west, reflecting the occurrence of hail producing storms along the dryline in the high plains into the Texas panhandle. Hail is also less frequently found over the southeast of the CONUS where lapse rates are generally lower (Cintineo et al. 2012). In addition, hail is reported more often that tornadoes, with a CONUS total frequency of 4191 large hail compared to 1007 tornado reports per year on average for the period 1979-2012. Assessments of hail for the United States have relied mainly on these observational databases of hail that are known to be problematic (Doswell et al. 2005; Changnon et al. 2009). Other approaches have considered remotely sensed observations of hail, using satellite cloud top temperatures related to large hail, or radar reflectivity derived maximum expected size of hail to produce short climatologies (Cintineo et al. 2012; Cecil and Blankenship 2012). However, changing technology in both radar output for the United States and satellites limit both of these methods to about the last decade. The satellite approach, while global in coverage, overestimates hail occurrence over the tropics where large hail is rarely observed (Knight and Knight 2001; Cecil and Blankenship 2012). The radar-derived climatology in contrast is limited by spatial extent to available radar sites, temporal period due to changing technology, and poor discrimination in radar post-processing algorithms for hail larger than 4.9cm (Cintineo et al. 2012).

Attempts to relate hail occurrence to the large-scale environment have generally focused on small regions utilizing synoptic composites (e.g Cao 2008) or station proximity analyses (e.g Edwards and Thompson 1998). More recently, empirical hail models have been applied to to estimate frequency or size from the environmental conditions (e.g Jewell and Brimelow 2009; Sanderson et al. 2014). A small number of studies have investigated univariate or linear discriminants for hail that assume the independent variables are normally distributed (e.g Manzato 2012; Eccel et al.

2012; Manzato 2013). These have mainly focused on thermodynamic variables over small regions, or covariates such as used by Brooks et al. (2003). While Brooks et al. (2003) have shown the functional dependence of severe thunderstorms occurrence on both thermodynamics and vertical wind shear, the estimation of the frequency of hail events over the CONUS using non-linear multivariate relationships that assume non-normal distributions have not been considered. This suggests that another approach is required to estimate the frequency of hail.

The motivation behind our development of a new index summarizing relationships between environment and hail occurrence is to provide a proxy to observations of hail using available reanalysis data. This index can then be applied to understand the sensitivity of hail to its formative environment on a climate scale for seasonal prediction or climate change projections over both the CONUS and other regions with more sparse observations. To produce the index, monthly averages of the environmental parameters are used, which do not reflect the large day to day and diurnal variability present in parameters favorable to severe weather. In this paper, however, we seek to model long climatological periods and have a greater interest in perturbations to the mean climate state. If, in a particular month a number of days have high values of a given parameter, then it is reasonable to expect that this will be represented to some extent in the value of the mean for that month (Tippett et al. 2014).

This paper is structured as follows; Section 2 describes the hail observations used for the climatology along with the North American Regional Reanalysis (NARR) used as a source of environmental data. Section 3 details the development of the statistical relationship relating the occurrence of hail to the large-scale environment and considers how it compares to other potential models. Sections 4 and 5 explore the seasonal, interannual and spatial characteristics of the climatology on both a CONUS wide and regional basis. Finally, in Section 6, the limitations of the index and our approach are discussed, and the future potential applications of this index outlined.

2. Data and Approach

a. Storm Data Hail

A $1^\circ \times 1^\circ$ gridded dataset of monthly hail occurrence was constructed based on the National Climate Data Centers Storm Data for the period 1979-2012 (Schaefer and Edwards 1999). We define the monthly hail occurrence for each grid box and month as the number of three-hourly periods (0Z-3Z, 3Z-6Z, etc.) with at least one report of 1 inch or larger hail. This definition means that any three hour period and grid box with one or more large hail reports counts as a single event. We chose this definition of a hail event, with its filtering in time and space, to reduce the influence of non-meteorological factors such as population and road distributions. Figure 2(a) shows as an example that near Amarillo, Texas reports of large hail have distinct small-scale spatial structure that is likely more related to road networks and population than meteorological variations. The clear imprint of the road network on hail reports suggests that simple corrections for report biases using population density alone are likely to be of limited effectiveness. However, the time and space filtering of the monthly hail event definition removes some of these influences and leaves a large scale east to west decrease in monthly hail occurrence (Figure 2(b)). This gradient coincides with a drop-off in population and road network density. The one inch threshold also serves to remove sampling and observer issues that result from quantized biases towards the minimum threshold (Schaefer et al. 2004). This definition had the greatest impact for the period 1979 to 2010, when the minimum reported hail threshold was 0.75 inches before its elevation to one inch in 2010.

We note that hail events as we have defined them here are utilized in the derivation of the index relationship between hail and its environment. Thus the spatial and temporal biases of the gridded hail events data are less important once the index has been defined. Thereafter, the climatology is estimated from the occurrence of hail as predicted by its environment, producing a degree of independence assuming a large enough initial sample is used to develop a robust relationship.

This also implies that the index relationship is less susceptible to non-meteorological trends in interannual variability or seasonality.

b. North American Regional Reanalysis

The North American Regional Reanalysis (NARR; Mesinger and Coauthors 2006) was chosen to provide environmental data for formulation of the index. The reanalysis has a horizontal resolution of 32 kilometers. For this application, the data were interpolated to a $1^\circ \times 1^\circ$ grid over the CONUS (25° - 50°N, 130° - 60°W), used for the hail observations. Twenty monthly mean parameters were chosen for testing in the index. These included thermodynamic and kinematic quantities, parameters commonly used for hail detection in an operational setting, as well as other parameters potentially related to the seasonal cycle (Table 1). In addition parameters relating to observational characteristics including $1^\circ \times 1^\circ$ gridded elevation and population were also considered.

A number of inadequacies are present in the NARR dataset, despite the aim of reanalysis to produce a closest to reality archive of the atmosphere. Wind fields and calculated measures of vertical wind shear have been shown to be well replicated, particularly outside of the planetary boundary layer where sub-grid scale influences become more important (Gensini et al. 2014). NARR thermodynamic quantities in contrast have been shown to have several limitations. The deficiencies in NARR thermodynamics partly relate to the activation of shallow convection within the Eta model convection scheme used to produce the reanalysis, which results in large amounts of drying between 900 and 700hPa and strongly influences the development of both instability and convective inhibition (Baldwin et al. 2002; Gensini et al. 2014; Tippett et al. 2014). However, for parameters such as convective precipitation, NARR could be potentially advantageous, as the assimilated precipitation can assist in damping activity in the model's convective scheme (Mesinger and Coauthors 2006; Bukovsky and Karoly 2007; Tippett et al. 2014).

3. Statistical Relationships

a. Poisson Regression

Several approaches have been used previously to fit statistical relationships between observed severe weather and its related environment (e.g. Brooks et al. 2003; Eccel et al. 2012; Elsner and Widen 2014). Here we use Poisson regression, which assumes a log-linear relationship between the severe weather parameters and the occurrence of hail. The standard generalized linear model for a Poisson regression is used (Wilks 2006) and is arranged to predict the expected number of hail events per month (μ). An offset term is used to account for the different area of each grid box and the number of years in the climatology, removing the dependence of the coefficients on grid resolution and climatology length. Importantly, the linear covariate relationship of Brooks et al. (2003); Brooks (2013) has shown that the functional dependence of severe thunderstorms is on the unequally weighted logarithm of both CAPE and S06. Thus, both of these parameters are provided to the fitting procedure to determine whether these parameters are relevant for large hail and the appropriate coefficients. We note however, that fitting the Poisson regression assumes an equal mean and variance, and thus the potential exists for over-dispersion (Elsner and Widen 2014).

The Poisson regression is fit by relating the monthly climatological frequency of hail to the monthly climatological values of the set of parameters listed in Table 1. The model attempts to estimate the number of hail events in a given month based on a determined set of monthly mean environmental parameters. The approach has previously been applied to both tropical cyclones (Tippett et al. 2011) and tornadoes (Tippett et al. 2012, 2014). One of the potential dangers of fitting any regression is over-fitting, where an excessive number of parameters representing the distribution present no benefit to the fit, or deviate from a physical reasoning. Over-fitting was avoided by increasing the number of parameters until the addition of further parameters results in minimal gain in performance. As in both previous applications, an increasing number of environmental parameters is chosen by a forward selection procedure. The coefficients minimize the

deviance, a measure of the goodness of fit. The mean and standard deviation of the deviance is computed from 10 iterations of 10-fold cross validation. Variables were also checked to ensure a log-linear coefficient relationship, and each of those found suitable had this characteristic, except for small values of the mean specific humidity between the surface (2m) and 90hPa above ground level (Q_{mean}), where the coefficients were positive (not shown). Exploring this spatially revealed that these small values only occur for a few grid points in the northern CONUS during January, February and March, where moisture limitation may be important. All other locations did not display this coefficient relationship to Q_{mean}.

To examine the contributions of the respective fitting parameters, each level of the fit inclusion was explored by visual inspection of maps of indices constructed from different subsets of parameters (Figure 3). cPrcp was the first parameter selected by the deviance minimisation of the forward selection procedure. Physically, cPrcp is a consequence of both convective initiation by the model and the thermodynamic instability present within the atmosphere. The magnitude of the resultant convective rainfall is constrained by assimilation of precipitation data in the NARR reanalysis. However, cPrcp alone does not produce a useful distribution for representing the occurrence of hail, with the peak values confined to the gulf coast and close to the source of moisture (Figure 3(a)). The two-parameter model, like that for tornadoes, includes SRH, with stronger amplitude shifted over the plains relative to the tornado climatology but with a similar set of coefficients (Table 2, Figure 5(c)). Again, the inclusion of SRH is physically reasonable, reflecting the potential for organized thunderstorms and rotating updrafts characteristic of supercells, the producers of a significant fraction of large hail. Adding a third parameter results in inclusion of a direct measure of the potential updraft strength, MLCAPE. Unlike cPrcp, which describes a model response to available energy and varies depending on the atmospheric moisture content and other factors, MLCAPE describes the potential energy available provided the model does not deplete available energy prior to the analysis time. As this parameter was calculated with a mixed-layer parcel depth of 180hPa, the deep parcel is also likely a reflection of the convective inhibition present within the

atmosphere, perhaps explaining the westward shift of the climatological maximum in the index in addition to the expected thermodynamic relationship. The 3-parameter model produces a greater hail frequency over the southern half of Texas compared to observations, but is improved compared to the 2-parameter model. We suspect that this is a result of convective inhibition being handled poorly by many reanalysis products including NARR as seen for combinations of CAPE and S06 in this area (Brooks et al. 2003; Gensini and Ashley 2011). The deviance is further minimized by the addition of a fourth parameter, Q_{mean} (Figure 3(d)). On a diurnal scale this parameter is representative of moisture in the boundary layer, and the potential for loading of precipitable water within the updrafts of storms. However, these characteristics are unlikely to be represented in the monthly fitted parameter.

This 4-parameter model provides the "best" fit of the observed climatology. Additional parameters did not substantially improve the fit (Figure 4(a)). The spatial distribution of the 4-parameter model produces a more accurate representation of hail events in the Texas panhandle, eastern New Mexico, and eastern Colorado. This is not to say that the 4-parameter model is the only fit with similarly minimized deviance owing to the spread obtained by cross-validating the sample using selections of the observations. The overlap between different four parameter models exists due to the size of the sample increasing the spread of the deviance, and parameters that slightly differently describe thermodynamic or kinematic quantities also being considered. Thus, the relationship chosen here is the preferred choice using the data to decide upon the constituent parameters of the relationship. Further discussion of the applicability of the fit is presented in Section 3b.

Fitting was carried out to the tenth parameter inclusion of all potential parameters to test the extent to which deviance could be improved without over-fitting (Figure 4(a)). The set of all possible four-parameter models was also cross-checked to ensure that the model choice was not influenced by the order of the forward parameter selection (not shown). Fitting the Poisson regression to

observed hail occurrence we obtain the coefficients and parameters for the hail index as:

$$\begin{aligned}\mu_{\text{Hail}}(\mathbf{x}) = \exp[&-10.18 + 0.97\log(\text{cPrcp}) + 1.13\log(\text{SRH}) \\ &+ 1.00\log(\text{MLCAPE}) - 0.31\text{Q}_{\text{mean}} + \log\left(\Delta x\ \Delta y\ T\cos\phi\right)]\end{aligned} \tag{1}$$

Where the final term is the spatio-temporal offset, with ϕ as the latitude, Δx and Δy are the longitude and latitude spacings in degrees, respectively, and T is the number of years. This new Hail Index reflects a significant difference from the tornado index (2), reflecting the different spatial distribution and environmental conditions that precede the respective thunderstorm phenomena. The tornado index by comparison is (Tippett et al. 2012, 2014):

$$\mu_{\text{Tornado}}(\mathbf{x}) = \exp\left[-10.59 + 1.36\log(\text{cPrcp}) + 1.89\log(\text{SRH}) + \log\left(\Delta x\ \Delta y\ T\cos\phi\right)\right] \tag{2}$$

While this relationship is not dissimilar to the 2-parameter Hail index, Figure 4(a) indicates that the deviance from the hail data is reduced significantly by addition of the third and fourth parameters. This was not the case for the tornado data, where using greater than 2 parameters did not improve the index fit. The index for tornadoes, in comparison to the four parameter hail index, has a greater dependence on SRH. This difference is expected, as tornadoes are more reliant than hail on the presence of low level environmental wind shear (Brooks et al. 2003). The importance of cPrcp is also reduced in the 4-parameter index, though this may be due to the lower spatial correlation between cPrcp and hail occurrences. Comparing to the 3-parameter index, the dependence on SRH decreases by almost a half (Table 2). Contrasting this, the dependence on MLCAPE doubles, while the dependence on cPrcp also increases by a third. These coefficient changes, together with the addition of Q_{mean}, improve the spatial distribution over the problematic southern Texas and coastal areas when compared to the 3-parameter hail index (Figures 5(a),5(b)). Q_{mean} however does not improve errors near the front-range of the Rocky mountains, which contradicts the expectation that additional moisture in this area would be favorable to the development of hail.

The correlation of Q_{mean} with the hail index and with the monthly hail occurrence data is positive and significant, which is physically sensible. It is therefore surprising that the coefficient

of Q_{mean} in the index is negative (Table 2). This behavior can be understood by noting that Q_{mean} is well-correlated with MLCAPE and cPrcp. The predictors exhibit co-linearity. Thus the sign of the coefficient of Q_{mean} must take into account the relation of Q_{mean} with hail occurrence and as well as its relation with the other predictors. Here, there is a negative relation between Q_{mean} and the variability unexplained by the first three predictors, and this relation results in a negative coefficient for Q_{mean} in the optimum four parameter fit.

b. Other Potential Models

Two other potential indices are presented for comparison to the hail climatology (Figures 5(c),5(d)). The first is the tornado index (Tippett et al. 2012, 2014). This comparison illustrates the novelty of the hail index, showing the clear differences between hail and tornado environmental relationships. While the tornado index is characterized by a double lobe structure of the so-called Tornado and Dixie alleys, hail occurrence is more confined to the central Great Plains. This presumably reflects the access to greater instability and steep mid-level lapse rates that is found in this region for storms, downstream of the high terrain, whereas by the time such air has moved over the east, it has typically been mixed by repeated days of convection, reducing these lapse rates and instability (Cintineo et al. 2012). We also compare to the 4-parameter index that does not include convective precipitation as one of the constituent parameters (Figure 5(d)). When ranked by minimised deviance, this corresponds to the 10th ranked index. The moisture quantity Q_{mean} is found in all ten of these indices, along with a range of shear and CAPE representations. This index with no cPrcp includes; MLCAPE, S06, the relative height of the lifted condensation level (rLCL) and Q_{mean}. However, like many of the CAPE-Shear product indices that have been applied for 6 hourly data (e.g. Brooks et al. 2003; Gensini and Ashley 2011), this model suffers from overly high values in the southern parts of Texas where climatological CAPE is high (thereby generating a high mean), but convection is rarely initiated. This reveals that including the NARR cPrcp in our

index reduces this problem similar to the results of Trapp et al. (2009), though does not remove it entirely (Figure 4(a)).

4. Interannual Totals and Variability

a. Correlations

To further evaluate the hail index, we compute the index from interannually varying monthly environmental parameters, and compute its deviance with respect to the interannually varying hail occurrence data (Table 2, Figure 4(b)). This test examines whether the index is capable of representing interannual variability, as the interannual data is independent of the data used to fit the index. The ratio of interannual deviance to the deviance of the index with climatological environments illustrates that deviance is reduced when using interannual environments (Figure 4(b)). This suggests that the index has predictive capability for independent data. To quantify the extent to which the interannual variability of each of the individual parameters contributes to that reduction in deviance, we compute the deviance of the interannually varying hail occurrence data with respect to a hail index, where only a single parameter varies interannually and the other three have climatological values. This was then computed as a ratio of deviance to the deviance calculated using climatological environments. For each of cPrcp, SRH and MLCAPE this resulted in the expected reduction in the ratio of deviance, supporting that the contribution of each parameter to the index improved the relationship. However, for Q_{mean}, this increased the deviance of the fit. This suggests that for the CONUS total, Q_{mean} does not improve the index performance when applied to interannual data. Testing this behavior of the parameter, the deviance with each of SRH, MLCAPE and cPrcp interannually varying was evaluated with the environmental climatological values of Q_{mean}. The reduction in deviance for this combination suggests that while climatological values of Q_{mean} do improve the fit, interannually varying values of Q_{mean} have limited if any predictive

316 value (Table 3).

317 The influence Q_{mean} has on the index was also explored by considering the correlations of
318 monthly frequency between the index and observations for each of the suppressed parameters
319 (Table 3). The index tested for interannual data shows significant correlation (T-test of 0.05) for
320 much of the year outside of late summer and early autumn. The greatest portion of variability in the
321 index can be explained by MLCAPE from November through April, with cPrcp also contributing
322 during both December and January. As the season approaches the transitional period of spring,
323 SRH plays a greater role for April through June, where instability is more commonly available,
324 but strong rotational potential for storms overlapping instability is less common. In comparison
325 to the other parameters, Q_{mean} shows poor correlations for the interannual data for much of the
326 winter and spring. This is, however, offset by positive correlations during the summer and early
327 fall. Comparing these using the 9 NOAA climate regions (Karl and Koss 1984), monthly frequency
328 correlations reveal that climatological Q_{mean} does have regionally positive skill on interannual data
329 for given months (Table 5). It is also possible that Q_{mean} does not vary greatly for monthly average
330 values which smooth much of the diurnal variability present.

331 *b. Annual Totals*

332 Artificial trends in observations are a considerable problem in the reported hail climatology
333 (Doswell et al. 2005). Despite this, recent work using normalized insurance losses and environ-
334 mental data has suggested increases to both frequency and variability of severe thunderstorm losses
335 due to changes in environments over the period 1970-2009 (Sander et al. 2013). Examining hail
336 events, a strong positive trend is found in the total annual occurrence over the CONUS (Figure
337 6). Similar to the inflation adjustment applied to tornado observations[2] (Tippett et al. 2012), the
338 observed large hail events are linearly de-trended to compare to the index annual totals. The results

[2]Details of this adjustment can be found at http://www.spc.noaa.gov/wcm/adj.html

of this correction can be seen in the adjusted observations. Correlations in annual total between the observations and the index increase from 0.22 for the raw observational data to 0.57 for the de-trended data. Variability in annual total appears to be well captured by the index and increases during the 2000s, with little apparent upward trend in annual frequency for the CONUS. Discrepancies between the index and observations in peak values may be related to the smoothing of the adjustment procedure or more localized environment characteristics leading to hail occurrence. While this adjustment is applicable to the CONUS total, the differences in remaining variance suggested that further analysis over smaller regions was warranted.

On a regional scale, large variations in the annual total number of hail events are also found. These trends are difficult to correct using simple de-trending, with increases of three to four times the number of hail events and discontinuities (not shown). In comparison, index values produce a more consistent record of the annual total number of hail events for each region, with little to no trend in all but the Plains, Southwest and the Northwest. In each of these regions, there appears to be a small negative trend. The presence of such large trends in the hail events makes evaluation of the ability of the index to represent trends in hail occurrence difficult, and highlights that caution must be taken when considering trends over large spatial areas, and when considering reports that are subject to non-meteorological factors. This suggests that alternative data sources, including other reanalyses, component ingredients and remote observations are necessary to understand whether such trends are artifacts of the dataset or an actual climatic signal.

c. Seasonal Totals

The climatologically fitted index has a similar seasonal cycle to that in observations, with reduced year-to-year variability and some deficiencies in the mean of the seasonal cycle (Figure 7). The main difference is a small underestimation of the occurrence of hail in the peak months of May through July, and a small overestimation for the autumnal months September through November.

These biases in the mean reflect two limitations of the index; in the western high plains of Colorado, the occurrence of hail over this area is underestimated by the index. A potential explanation is the reduced moisture in the NARR reanalysis compared to observations over Colorado which impacts the values of Q_{mean}, cPrcp and MLCAPE (Gensini et al. 2014). The second problem arises over the southeast of the continent, where the index is also biased downwards. The extent to which this is a real bias as compared to an observational flaw arising from the verification process may be questionable (Cintineo et al. 2012). As would be expected, the variability of the climatologically fitted index is smaller owing to reduced capability to capture seasonal variations, however a large portion of sample falls within the expected range. While the index does have limitations in its handling of the variability, it shows a capability to simulate the extreme outliers of the climatology (e.g. April).

While continent-wide analysis indicates that the index has the capability to capture the seasonal cycle of hail occurrence, regionally the index may not reflect all potential hail producing environments. This characteristic is related to the frequency of occurrence of the constituent ingredients over different parts of the continent, and how these coincide (Brooks 2009). The index performs well in estimating the timing of the seasonal peak for all of the eight NOAA climate regions considered except the northwest, which only constitutes a small fraction of the observed reports (Figure 8). Three different behaviors can be seen in the difference between the index and observations over the respective regions; Central Plains (South, Central, Plains), East (Southeast and Northeast) and West (Upper Midwest, Southwest). In the central plains, both peak magnitude and the timing of the seasonal cycle are well replicated (Figure 8(a),8(d),8(f)). Given that a large fraction of CONUS hail occurrence is found in these regions, it is not surprising that the index would capture the seasonal cycle well in these regions, though the spread of variability is less in the index for both the Central and Plains regions. Despite this decreased spread in interannual variability, correlations of frequency for these regions on a monthly scale show appreciable skill for the peak months of the climatology (Table 4).

Over the east of the CONUS, both the temporal structure and the summer peak of the seasonal cycle is replicated. However, the magnitude of the index is much lower than the observed frequencies (Figure8(b),8(c)). These underestimates are potentially related to the buoyancy-driven environments in which these storms occur, or possible biases in the reporting arising from warning verification policy (Cintineo et al. 2012). Despite this poor representation of the seasonal cycle and variability, significant correlations are found for all but October and December in the Northeast, with the highest values during spring and the early summer (Table 4). In both the Upper Midwest and Southwest (Figure 8(e),8(g)), the index simulates the peak, but does not identify the decreasing frequency of hail in the late summer and early fall. This is again reflected in poor interannual correlations between observations and the index for all months barring October in these regions. Combining both the second and third characteristics reveals that the biases in the CONUS mean annual frequency arise from regions outside of the peak climatological frequency in the center of the CONUS, and suggest that regional examination of appropriate fits may be necessary to form a more precise climatology.

5. Spatial Maps

a. Annual

Despite the filtering and gridding procedures used here, the climatology of hail events continues to show biases towards urban centers and frequently traversed road networks as described in Section 2. The highest mean annual frequencies are found through northern Texas through Oklahoma and Kansas into southern Nebraska, with peak values between 10 and 11 hail events per year (Figure 9(b)). A northwestward extension occurs along the margins of the high terrain, reflecting the high frequency of hail at this altitude, while extension east is through the Missouri, Mississippi and Ohio valleys in one belt, and a second south of the Ozark Plateau and the Appalachian

mountains through the south to the Carolinas.

In contrast, the maximum in the index climatology is more confined to the plains, extending from the Rio Grande valley on the Mexican border northwards into southern Nebraska (Figure 9(a)). The spatial peak is found over northwestern and central Texas, extending through central Oklahoma and into southern Kansas, east as far as the Arkansas border and west to New Mexico. Despite the systematic bias in frequency when compared to the observed climatological frequency of hail events (Figure 5(a)), the index has an RMSE of 1.27 hail events annually, corresponding to less than 15% of the peak magnitude of 10 events and a pattern congruence of 0.93. While significant spatial biases compared to observations are found for the western parts of the plains (including eastern Colorado, northwestern Texas and eastern New Mexico), these differences are related to the relatively sparse population in these areas (Figure 2(b) and Changnon et al. (2009)), rather than indicating that environments favourable to hail events do not occur in these areas. Gridded population and elevation were also considered for their predictive capabilities in the index for this reason, but neither were selected. For population, the relationship with reports was not useful for areas where population exceeded more than one person per square kilometer, corresponding to much of the area east of the Rocky mountains. While below this threshold population density shows some skill, the distribution of hail frequency overlies areas with both little and greater population, thus reducing its effectiveness. In combination with the smoothing applied for the hail events to the $1^\circ \times 1^\circ$ grid that demonstrates the complex spatial relationships with reported hail, these factors explain why population was not effective as a predictand.

Peak frequencies in the index have similar magnitudes to the mean annual observational values, suggesting that this characteristic is well captured (Figure 9(a)). The northern extension along the Ohio valley to the east is present in the index climatology, but is displaced slightly southward. However, the index does not represent the climatological frequency over the southeast. The origins of large hail in this area may be related to the warning verification process, with hail climatologically less frequent in the area due to a reduced occurrence of high mid-level lapse rates and a

predisposition to greater updraft moisture loading (Cintineo et al. 2012). Additionally, a large part of the frequency, particularly further east, may reflect the occurrence of pulse-type thunderstorms during the summer months rather than the likelihood of organized storms that the index attempts to identify. Given that these storms are primarily driven by thermodynamic and buoyancy processes rather than vertical wind shear, and are inherently difficult to forecast on a diurnal timeframe, it is unsurprising that they are not identified by the index which assesses monthly mean conditions.

Subjective testing of index performance was also considered by calculating the mean annual frequency for the 2007-2010 period (not shown) used by Cintineo et al. (2012). The distribution was found to be similar both in terms of peak frequency and spatial extent to the radar-derived climatology, although the peaks around radar observation areas were not replicated, and the index was biased eastward. This suggests that in lieu of remotely sensed observations due to changing technologies, an index is a useful approach to estimate climatologies of hail.

b. Seasonal

A key test of the hail climatology is the handling of the progression of the seasonal cycle and its spatial variability. The spatial distributions of the climatology were broken down to consider the spring (MAM) and summer (JJA) periods (Figure 10). For MAM, the index performed similarly to the performance for the full year, with the relative RMSE of a similar value (Table 6). There is a slight bias towards the southeast, an overestimation near the Gulf coast and Mexican border, and deficiencies in frequency over the southeast (Figure 10(b)). The biases in southern Texas in the index, while improved relative to those identified using purely CAPE and Shear parameters (e.g. Brooks et al. 2003; Gensini and Ashley 2011) suggest that the question of initiation remains a problem in the statistical downscaling of environments.

During the summer months, the index correctly shifts the spatial distribution northwest, while decreasing the intensity (Figure 10(c)). In comparison to observations, there is a pronounced

eastward bias resulting from moisture deficiencies closer to the Rockies, with lower frequency also found in the east (Figure 10(d)). The deficiency in the index for the Colorado high plains, a region known to have some of the highest frequencies of hail occurrence, is also problematic for the index (Changnon et al. 2009). This deficiency likely arises from a low bias in moisture in the reanalysis as suggested by Gensini et al. (2014), and perhaps environments with a weaker dependence on SRH where mesoscale influences may offset the reduced values of this parameter (Wakimoto and Wilson 1989).

Another way to evaluate the seasonal cycle in the index is to identify the peak month of climatological frequency in the index as compared to the observations (Figure 11). Spatially, the peak of season observation distribution shifts from the Gulf coast to the southern plains of Oklahoma in April and May, before shifting to the north and west during June and reaching the most northern margins of the continent by July. Overall, the index is found to perform well in replicating the shift to the northwest that occurs between the early spring in the southeast and summer over the high plains. However, the index peaks later than observations in the west. The peak month in the northeast for the index also differs compared to observations, occurring in June rather than July, while the index also suggests a peak in Florida in the early spring when in observations this is found in the summer months. Surprisingly, the index appears to identify the hail peak in the southwest, associated with the tail end of the monsoonal pattern when moisture below 700hPa is high (Maddox et al. 1995). It is also noted that over the area west of the Rocky Mountains where few observations exist, the index pattern does not reproduce the sporadic observational peaks, despite the losses in this area (Changnon et al. 2009).

6. Conclusions

A new index for the monthly occurrence of large hail (greater than one inch in diameter) was developed using a Poisson regression to relate environmental parameters to hail events. Hail events

are defined by the number of three-hourly periods in a month that produce one or more reported occurrences of hail greater than one inch in a $1^\circ \times 1^\circ$ grid box. The index involves convective precipitation, storm relative helicity between the surface and three kilometers, 180hPa mixed-layer CAPE and mean specific humidity in the lowest 90hPa of the atmosphere. The index differs in its choice of parameters and their weighting from existing indices for tornadoes (Tippett et al. 2012, 2014), and indices that were developed using multiple types of severe weather (Brooks et al. 2003; Gensini and Ashley 2011; Allen and Karoly 2014). It is important to note however, that this model fits large hail, whereas prior studies generally examined hail in excess of two inches.

The performance of the hail index in terms of both regional and spatial seasonality and frequency was explored. The Q_{mean} parameter improves index performance for climatological data and has a positive correlation with both the index and observed hail events. However, Q_{mean} has a negative coefficient in the index, which can be explained due to the parameters co-linearity with the other predictors that are also fitted in the relationship with hail occurrence. Testing on interannual data revealed little skill for Q_{mean} as a seasonal predictand. The largest influences of Q_{mean} on the index were found for areas near the gulf coast and in regions where moisture rapidly retreats southward during the fall. The index performs well in showing the spatial shifts of the climatological distribution of large hail over the year, with some problems in simulating variability, particularly during the summer where underestimation occurs, and during fall where the index does not decrease sufficiently. This representation of the seasonal cycle is found to be regionally best from the South to Central Plains and through the Midwest. The index does not capture the westward shift in peak frequency early enough, which appears to be related to moisture biases in the NARR product. In terms of annual total frequency, the index produces a realistic annual climatology of occurrence unlike the large trends found in observations on a continental scale. However, if observed hail data is de-trended, the resulting inflation adjusted hail frequency is similar to the index. However, remaining differences in variance and variability of the seasonal cycle suggest further analysis of these trends on smaller regional scales is necessary. This analysis should examine environmental

parameters, other observations (e.g. tornadoes, lightning) and component indices to understand both the flaws in the observational data, and potential trends in climatic conditions.

It is important to note that while the index is selected as a best fit to the observational data, there are clearly physical relationships between observations of hail and the index on the monthly scale owing to the parameters chosen. While the model here is chosen to minimize deviance, it is a single model that fits the data, and does not preclude other models that may also have a similar range of deviance (or similar ingredients). Examples of this include related models identified by our procedure as the next best candidates from the data, or those derived from approaches using other generalized linear models or regressions to estimate the coefficients (e.g. Eccel et al. 2012; Elsner and Widen 2014). Another limitation of the index is that monthly data is clearly removed from the diurnal variability of the component ingredients and parameters favorable to convection. However, occurrences of large hail are related to environments that occur at the extremes of all thermodynamic and kinematic environments, and shifts in these outlying values may have some expression in the mean monthly values. The use of monthly average environments limits applicability to months that see a significant perturbation of the mean, rather than a single isolated event. While these limitations may make the index less relevant to large hail forecasting, the longer term averages are better replicated by seasonal forecast models, one of the intended applications of the index. Despite these limitations, the index appears to agree well with ongoing projects to supplement the observational data using remote sensing sources such as radar (Figures 9 and 11 of Cintineo et al. (2012)), with similar spatial and seasonal frequency despite the relatively limited temporal climatology in that study.

Future applications of the index include use with other reanalysis datasets to explore the sensitivity to the model configuration and elevated hail size thresholds, and estimates of potential climate changes or seasonal forecast. Sub-daily and daily data will also be explored, particularly with reference to forecast applications of the index and as a way of generating proxy risk assessments over the continental United States.

Acknowledgments.

The authors are supported by grants from the National Oceanic and Atmospheric Administration (NA05OAR4311004 and NA08OAR4320912), the Office of Naval Research (N00014-12-1-0911) and a Columbia University Research Initiatives for Science and Engineering (RISE) award. The views expressed herein are those of the authors and do not necessarily reflect the views of NOAA or any of its sub-agencies.

REFERENCES

Allen, J. T. and D. J. Karoly, 2014: A climatology of Australian severe thunderstorm environments 1979-2011: Inter-annual variability and ENSO influence. *Int. J. Climatol.*, **34**, 81–97.

Baldwin, M. E., J. S. Kain, and M. P. Kay, 2002: Properties of the convection scheme in NCEP's Eta Model that affect forecast sounding interpretation. *Wea. Forecasting*, **17**, 1063–1079.

Blair, S., D. E. Cavanaugh, J. Laflin, J. Leighton, and K. Sanders, 2014: High-resolution hail observations: Implications for NWS warning operations and climatological data. *26th Conf. on Weather Analysis and Forecasting, Atlanta, GA, Amer. Meteor. Soc.*

Brooks, H. E., , J. W. Lee, and J. P. Craven, 2003: The spatial distribution of severe thunderstorm and tornado environments from global reanalysis data. *Atmos. Res.*, **67**, 73–94.

Brooks, H. E., 2009: Proximity soundings for severe convection for Europe and the United States from reanalysis data. *Atmos. Res.*, **93**, 546–553.

Brooks, H. E., 2013: Severe thunderstorms and climate change. *Atmos. Res.*, **123**, 129–138.

Bukovsky, M. S. and D. J. Karoly, 2007: A brief evaluation of precipitation from the North American regional reanalysis. *J. Hydrometeor.*, **8**, 837–846.

Cao, Z., 2008: Severe hail frequency over Ontario, Canada: Recent trend and variability. *Geophys. Res. Lett.*, **35**, L14 803, doi:10.1029/2008GL034888.

Cecil, D. J. and C. B. Blankenship, 2012: Toward a global climatology of severe hailstorms as estimated by satellite passive microwave imagers. *J. Climate*, **25**, 687–703.

564 Changnon, S. A., 1999: Data and approaches for determining hail risk in the contiguous United
565 States. *J. Appl. Meteor.*, **38**, 1730–1739.

566 Changnon, S. A., 2008: Temporal and spatial distributions of damaging hail in the continental
567 United States. *Phys. Geography*, **29**, 341–350.

568 Changnon, S. A., D. Chagnon, and S. D. Hilberg, 2009: *Hailstorms across the nation: An atlas*
569 *about hail and its damages*. Illinois State Water Survey, 95pp.

570 Cintineo, J. L., T. M. Smith, V. Lakshmanan, H. E. Brooks, and K. L. Ortega, 2012: An objective
571 high-resolution hail climatology of the contiguous United States. *Wea. Forecasting*, **27**, 1235–
572 1248.

573 Craven, J. P., R. E. Jewell, and H. E. Brooks, 2002: Comparison between observed convective
574 cloud-base heights and lifting condensation level for two different lifted parcels. *Wea. Forecast-*
575 *ing*, **17**, 885–890.

576 Davis, S. M. and J. LaDue, 2004: Nonmeteorological factors in warning verification. *Preprints,*
577 *22nd Conf. on Severe Local Storms, Hyannis, MA, Amer. Meteor. Soc., CD-ROM P*, Vol. 7, 4pp.

578 Doswell, C. A., 2007: Small sample size and data quality issues illustrated using tornado occur-
579 rence data. *Electronic J. Severe Storms Meteor.*, **2**, 1–16.

580 Doswell, C. A., III, H. E. Brooks, and M. P. Kay, 2005: Climatological estimates of daily local
581 nontornadic severe thunderstorm probability for the United States. *Wea. Forecasting*, **20**, 577–
582 595.

583 Doswell III, C. A. and P. M. Markowski, 2004: Is buoyancy a relative quantity? *Mon. Wea. Rev.*,
584 **132**, 853–863.

585 Eccel, E., P. Cau, K. Riemann-Campe, and F. Biasioli, 2012: Quantitative hail monitoring in an
586 alpine area: 35-year climatology and links with atmospheric variables. *Int. J. Climatol.*, **32**,
587 503–517.

588 Edwards, R. and R. L. Thompson, 1998: Nationwide comparisons of hail size with WSR-88D
589 vertically integrated liquid water and derived thermodynamic sounding data. *Wea. Forecasting*,
590 **13**, 277–285.

591 Elsner, J. B. and H. M. Widen, 2014: Predicting spring tornado activity in the central Great Plains
592 by 1 March. *Mon. Wea. Rev.*, **142**, 259–267.

593 Gensini, V. A. and W. S. Ashley, 2011: Climatology of potentially severe convective environments
594 from the North American regional reanalysis. *Electronic J. Severe Storms Meteor.*, **6**, 1–40.

595 Gensini, V. A., T. L. Mote, and H. E. Brooks, 2014: Severe thunderstorm reanalysis environments
596 and collocated radiosonde observations. *J. Appl. Meteor. Climatol.*, **In Press**, doi:http://dx.doi.
597 org/10.1175/JAMC-D-13-0263.1.

598 Grams, J. S., R. L. Thompson, D. V. Snively, J. A. Prentice, G. M. Hodges, and L. J. Reames,
599 2012: A climatology and comparison of parameters for significant tornado events in the United
600 States. *Wea. Forecasting*, **27**, 106–123.

601 Groenemeijer, P. and A. Van Delden, 2007: Sounding-derived parameters associated with large
602 hail and tornadoes in the Netherlands. *Atmos. Res.*, **83**, 473–487.

603 Hales Jr, J. E., 1993: Biases in the severe thunderstorm data base: Ramifications and solutions.
604 *Preprints, 13th Conf. on Weather Forecasting and Analysis, Vienna, VA, Amer. Meteor. Soc*,
605 504–507.

606 Jewell, R. and J. Brimelow, 2009: Evaluation of Alberta hail growth model using severe hail
607 proximity soundings from the United States. *Wea. Forecasting*, **24**, 1592–1609.

Karl, T. R. and W. J. Koss, 1984: Regional and national monthly, seasonal, and annual temperature weighted by area, 1895-1983. Historical climatology series 4-3, National Climatic Data Center, Asheville, NC. 38 pp.

Kelly, D. L., J. T. Schaefer, and C. A. Doswell III, 1985: Climatology of nontornadic severe thunderstorm events in the United States. *Mon. Wea. Rev.*, **113**, 1997–2014.

Knight, C. A. and N. C. Knight, 2001: Hailstorms. *Severe Convective Storms, Meteorological Monographs*, **28**, 223–248.

Maddox, R. A., D. M. McCollum, and K. W. Howard, 1995: Large-scale patterns associated with severe summertime thunderstorms over central Arizona. *Wea. Forecasting*, **10**, 763–778.

Manzato, A., 2012: Hail in northeast Italy: Climatology and bivariate analysis with the sounding-derived indices. *J. Appl. Meteor. Climatol.*, **51**, 449–467.

Manzato, A., 2013: Hail in northeast Italy: A neural network ensemble forecast using sounding-derived indices. *Wea. Forecasting*, **28**, 3–28, doi:http://dx.doi.org/10.1175/WAF-D-12-00034.1.

Mesinger, F. and Coauthors, 2006: North American Regional Reanalysis. *Bull. Am. Meteor. Soc.*, **87**, 343–360.

Ortega, L., T. M. Smith, K. L. Manross, K. A. Scharfenberg, A. Witt, A. G. Kolodziej, and J. J. Gourley, 2009: The severe hazards analysis and verification experiment. *Bull. Am. Meteor. Soc.*, **90**, 1519–1530.

Sander, J., J. F. Eichner, E. Faust, and M. Steuer, 2013: Rising variability in thunderstorm-related U.S. losses as a reflection of changes in large-scale thunderstorm forcing. *Wea. Climate Soc.*, **5**, 317–331, doi:doi:http://dx.doi.org/10.1175/WCAS-D-12-00023.1.

Sanderson, M., W. Hand, P. Groenemeijer, P. Boorman, J. Webb, and L. McColl, 2014: Projected changes in hailstorms during the 21st century over the UK. *Int. J. Climatol.*, **In Press**, doi: 10.1002/joc.3958.

Schaefer, J. T. and R. Edwards, 1999: The SPC Tornado/Severe Thunderstorm Database. *Preprints, 11th Conf. Applied Climatology*, Dallas, TX, Amer. Meteor. Soc., 215–220.

Schaefer, J. T., J. J. Levit, S. J. Weiss, and D. W. McCarthy, 2004: The frequency of large hail over the contiguous United States. *Preprints, 14th Conf. Applied Climatology, Seattle, WA, Amer. Meteor. Soc*, 7pp.

Stumpf, G. J., T. Smith, and J. Hocker, 2004: New hail diagnostic parameters derived by integrating multiple radars and multiple sensors. *Preprints, 22nd Conf. on Severe Local Storms, Hyannis, MA, Amer. Meteor. Soc., CD-ROM P7.8.*

Thompson, R. L., B. T. Smith, J. S. Grams, A. R. Dean, and C. Broyles, 2012: Convective modes for significant severe thunderstorms in the contiguous United States. Part II: Supercell and QLCS tornado environments. *Wea. Forecasting*, **27**, 1136–1154.

Tippett, M. K., S. J. Camargo, and A. H. Sobel, 2011: A Poisson regression index for tropical cyclone genesis and the role of large-scale vorticity in genesis. *J. Climate*, **24**, 2335–2357.

Tippett, M. K., A. H. Sobel, and S. J. Camargo, 2012: Association of U.S. tornado occurrence with monthly environmental parameters. *Geophys. Res. Lett.*, **39**, L02 801.

Tippett, M. K., A. H. Sobel, S. J. Camargo, and J. T. Allen, 2014: An empirical relation between U.S. tornado activity and monthly environmental parameters. *J. Climate*, **In Press**, doi:http://dx.doi.org/10.1175/JCLI-D-13-00345.1.

Trapp, R. J., N. S. Diffenbaugh, and A. Gluhovsky, 2009: Transient response of severe thun-

derstorm forcing to elevated greenhouse gas concentrations. *Geophys. Res. Lett.*, **36**, L01 703, doi:10.1029/2008GL036203.

Trapp, R. J., D. M. Wheatley, N. T. Atkins, R. W. Przybylinski, and R. Wolf, 2006: Buyer beware: Some words of caution on the use of severe wind reports in postevent assessment and research. *Wea. Forecasting*, **21**, 408–415.

Wakimoto, R. M. and J. W. Wilson, 1989: Non-supercell tornadoes. *Mon. Wea. Rev.*, **117**, 1113–1140, doi:10.1175/1520-0493(1989)117⟨1113:NST⟩2.0.CO;2.

Wilks, D. S., 2006: *Statistical methods in the atmospheric sciences*, Vol. 59. Academic Press, 627 pp.

Wyatt, A. and A. Witt, 1997: The effect of population density on ground-truth verification of reports used to score a hail detection algorithm. *Preprints, 28th Conf. on Radar Meteorology, Austin, TX, Amer. Meteor. Soc.*, 368–369.

List of Tables

1 List of parameters chosen for relationship selection. Italics denote modelled parameters. LAPSE, S01, S06, S08, S6TP were all calculated using the respective temperature or wind fields at given layers. LCL height was calculated following the approach of Craven et al. (2002) for a mixed layer parcel and scaled using relative height from ground in hPa. Moisture means MeanRHZero and Q_{mean} were calculated using relative and specific humidity from the surface (2m) to the zero degree isotherm and 90hPa above the surface respectively. 31

2 Coefficients for Poisson regression models with increasing number of parameters and standard errors for coefficients. 32

3 Correlation between the index and reported number of hail events greater than one inch with all parameters climatological except the listed which is allowed interannually vary. Significant correlations are in bold. 33

4 Correlation between the index and reported number of hail events greater than one inch by U.S. climate region and month for the period 1979-2012. Significant correlations are in bold font. Regions and months with less than 34 reported hail events during the period are omitted. 34

5 As for Table 4 except correlation between the index with Q_{mean} fixed to climatology while other parameters are allowed to vary interannually and hail events greater than one inch by U.S. climate region and month for the period 1979-2012. 35

6 Root mean squared error and pattern congruence (uncentered pattern correlation, Wilks (2006)) for the hail index as compared to observed large hail events for the entire calendar year and the respective seasons. 36

Input Parameters	Abbrev.
0-3km Storm Relative Helicity	*SRH*
500hPa Temperature	*T500*
700-500hPa Lapse Rate	LAPSE
180hPa MLCAPE	*MLCAPE*
180hPa MLCIN	*MLCIN*
Convective Precipitation	*cPrcp*
Surface-Based CAPE	*SBCAPE*
Surface-Based CIN	*SBCIN*
Average SB and ML CAPE	AVGCAPE
Average SB and ML CIN	AVGCIN
0-1 km Bulk Wind Shear	S01
0-6 km Bulk Wind Shear	S06
0-8 km Bulk Wind Shear	S08
6km to Tropopause Wind Shear	S6TP
Relative Height of LCL	rLCL
Mixed-Layer LCL	MLLCL
Surface Equivalent Pot. Temp.	ThetaE
Mean RH Surf. to Zero Isotherm	MeanRHZero
Mean 2m to 90hPa Specific Humidity	Q_{mean}
Soil Moisture in 1m layer	*SoilM01*

TABLE 1. List of parameters chosen for relationship selection. Italics denote modelled parameters. LAPSE, S01, S06, S08, S6TP were all calculated using the respective temperature or wind fields at given layers. LCL height was calculated following the approach of Craven et al. (2002) for a mixed layer parcel and scaled using relative height from ground in hPa. Moisture means MeanRHZero and Q_{mean} were calculated using relative and specific humidity from the surface (2m) to the zero degree isotherm and 90hPa above the surface respectively.

Coefficients	Intercept	cPrcp	SRH	MLCAPE	Q_{mean}
1 Param.	-2.33±0.05	1.10±0.01	-	-	-
2 Param.	-10.07±0.14	1.48±0.03	1.86±0.01	-	-
3 Param.	-14.88±0.16	0.72±0.03	2.03±0.01	0.51±0.02	-
4 Param.	-10.33±0.17	0.99±0.03	1.14±0.02	1.00±0.02	-0.31±0.01
Tornado	-10.59±0	1.36±0	1.89±0	-	-

TABLE 2. Coefficients for Poisson regression models with increasing number of parameters and standard errors for coefficients.

	Jan	Feb	Mar	Apr	May	Jun	Jul	Aug	Sep	Oct	Nov	Dec	Ann
4-Param	**0.85**	**0.66**	**0.61**	**0.66**	**0.44**	**0.42**	-0.10	-0.10	-0.03	0.32	**0.63**	**0.44**	0.22
SRH	0.19	0.04	0.07	**0.42**	**0.47**	**0.39**	**0.35**	0.29	0.01	0.02	**0.35**	0.22	**0.47**
MLCAPE	**0.82**	**0.60**	**0.72**	**0.52**	**0.46**	0.05	-0.19	**-0.42**	-0.15	**0.39**	**0.57**	**0.39**	0.16
cPrcp	**0.76**	0.31	0.34	**0.37**	-0.33	0.04	-0.14	-0.17	-0.01	0.10	0.28	**0.50**	-0.29
Q_{mean}	**-0.40**	**-0.42**	**-0.42**	**-0.39**	-0.12	0.12	0.21	0.36	0.20	0.00	0.01	-0.05	0.13
Cl. Q_{mean}	**0.85**	**0.69**	**0.67**	**0.66**	**0.41**	**0.37**	-0.05	-0.23	-0.01	0.23	**0.47**	**0.35**	0.26

TABLE 3. Correlation between the index and reported number of hail events greater than one inch with all parameters climatological except the listed which is allowed interannually vary. Significant correlations are in bold.

	Jan	Feb	Mar	Apr	May	Jun	Jul	Aug	Sep	Oct	Nov	Dec	Ann
US Wide	**0.85**	**0.66**	**0.61**	**0.66**	**0.44**	**0.42**	-0.10	-0.10	-0.03	0.32	**0.63**	**0.44**	0.22
South	**0.81**	**0.77**	**0.44**	**0.65**	**0.41**	**0.54**	**0.59**	**0.47**	**0.39**	**0.36**	**0.69**	**0.43**	**0.35**
Southeast	**0.61**	0.29	**0.52**	**0.54**	**0.40**	0.07	0.03	0.32	0.00	0.05	**0.51**	**0.36**	0.11
Central	**0.77**	**0.51**	**0.81**	**0.72**	**0.72**	**0.76**	0.24	0.22	0.30	**0.43**	**0.36**	0.34	**0.70**
Upper MW	**0.59**	**0.42**	**0.79**	**0.51**	**0.81**	**0.48**	0.33	0.06	0.31	**0.48**	**0.50**	0.00	**0.38**
Plains	0.05	**0.43**	**0.65**	**0.55**	**0.58**	**0.42**	0.25	0.22	**0.35**	**0.63**	0.29	0.02	0.06
Northeast	**0.61**	**0.37**	**0.48**	**0.79**	**0.71**	**0.63**	**0.35**	**0.34**	**0.57**	0.16	**0.48**	0.21	**0.70**
Southwest	0.13	0.15	0.23	0.00	0.03	0.05	-0.20	-0.02	-0.04	**0.46**	0.31	-	**-0.48**
Northwest	-	-0.05	0.07	**0.35**	**0.40**	0.08	**0.38**	0.04	**0.41**	**0.40**	-	-	0.05
West	0.32	0.06	-0.16	**0.58**	0.26	**0.45**	0.08	0.17	0.18	**0.44**	0.10	-0.03	-0.06

TABLE 4. Correlation between the index and reported number of hail events greater than one inch by U.S. climate region and month for the period 1979-2012. Significant correlations are in bold font. Regions and months with less than 34 reported hail events during the period are omitted.

	Jan	Feb	Mar	Apr	May	Jun	Jul	Aug	Sep	Oct	Nov	Dec	Ann
US Wide	**-0.40**	**-0.42**	**-0.42**	**-0.39**	-0.12	0.12	0.21	0.36	0.20	0.00	0.01	-0.05	0.13
South	**0.83**	**0.79**	**0.41**	**0.63**	**0.28**	**0.45**	**0.52**	**0.34**	0.27	0.24	**0.55**	**0.37**	0.26
Southeast	**0.60**	0.25	**0.59**	**0.56**	**0.46**	0.06	-0.01	0.29	-0.13	-0.07	0.29	0.24	0.22
Central	**0.74**	**0.50**	**0.87**	**0.72**	**0.75**	**0.76**	0.13	0.17	0.18	**0.40**	0.30	0.31	**0.73**
Upper MW	**0.61**	**0.41**	**0.67**	**0.48**	**0.75**	**0.47**	0.25	0.04	0.30	0.43	0.52	0.00	0.40
Plains	0.08	**0.46**	**0.66**	**0.57**	**0.50**	**0.34**	0.37	0.16	**0.38**	**0.64**	0.23	0.02	0.11
Northeast	**0.70**	**0.39**	**0.53**	**0.79**	**0.76**	**0.66**	**0.35**	0.25	**0.64**	0.05	**0.52**	0.19	**0.77**
Southwest	0.18	0.15	0.24	0.02	0.02	-0.11	-0.16	-0.11	-0.05	**0.45**	0.28	-	-0.45
Northwest	-	-0.03	0.05	**0.40**	**0.42**	0.15	**0.44**	0.05	**0.51**	**0.41**	-	-	0.12
West	0.21	0.03	-0.19	**0.65**	0.24	**0.47**	-0.07	0.15	0.19	**0.47**	0.14	-0.01	-0.08

TABLE 5. As for Table 4 except correlation between the index with Q_{mean} fixed to climatology while other parameters are allowed to vary interannually and hail events greater than one inch by U.S. climate region and month for the period 1979-2012.

	Annual	DJF	MAM	JJA	SON
RMSE	1.27	0.22	0.76	0.88	0.35
Pattern Cong.	0.93	0.76	0.91	0.88	0.85

TABLE 6. Root mean squared error and pattern congruence (uncentered pattern correlation, Wilks (2006)) for the hail index as compared to observed large hail events for the entire calendar year and the respective seasons.

List of Figures

1 a) Annual mean number of gridded ($1^\circ \times 1^\circ$) reports of hail equal to or greater than 1 inch 1979-2012, and b) Annual mean number of gridded ($1^\circ \times 1^\circ$) reports of tornadoes greater than F0 intensity for the same period. 39

2 a) Point reports of hail over the period 1979-2012 for the Texas panhandle and surrounding areas bounded by 34° to 38°N and 96° to 100°W from NCDC Hail observations, and b) Total number of gridded ($1^\circ \times 1^\circ$) three hourly hail events ($\geq$1 inch) for the same period and domain. 40

3 Optimal deviance fitted Poisson regression indices for large hail events with increasing number environmental of parameters for the period 1979-2012. a) One parameter index (cPrcp), b) Two parameter index (cPrcp, SRH), c) Three parameter index (cPrcp, SRH, MLCAPE) and d) Four parameter index (cPrcp, SRH, MLCAPE, Qmean). Units are mean annual number of three hourly periods with hail events greater than one inch. 41

4 a) Deviance of index fit for increasing number of environmental parameters. b) Contribution of the respective parameters to index deviance measured as a ratio of deviance using the interannually varying parameter to the climatological value. 42

5 a) Difference between the mean annual number of 3-hourly periods with hail events for the four parameter hail index and observed large hail events 1979-2012. b) As for a), except difference between mean annual number of the three parameter hail index events and observed large hail events. c) Mean annual number of three hourly periods with tornado events from the tornado index calculated using Eqn.2 for the same period. d) Mean annual number of large hail events of the 'next best' index without cPrcp included. 43

6 Variability in annual CONUS total of hail events as compared to the index for the period 1979-2012. Grey line shows occurrence of large hail events over the respective regions, while the black line shows the annual frequency as simulated by the 4-parameter hail index. The adjusted observations (dashed grey) have been linearly detrended (trend shown in dashed black). 44

7 Seasonal variability of the hail index for total monthly hail events over the CONUS as compared to observed hail events 1979-2012. Lines are mean index (grey) and observations (black) seasonal cycle, whiskers reflect 2.7σ of the distribution (99.3 percent). Dots show outlying years which are outside the 2.7σ range. 45

8 As for Figure 7, except seasonal cycle of the index and observed hail events over the NOAA climate regions for a) South, b) Southeast, c) Northeast, d) Central, e) Upper Midwest, f) Plains, g) Southwest and h) Northwest. No outliers are shown. 46

9 a) Mean annual number of 3-hourly periods with large hail events as predicted by the four parameter index 1979-2012. b) As for a) except the mean annual occurrence of large hail events. 47

10 Seasonal mean number of 3-hourly periods with large hail events from the four parameter index 1979-2012 for a) March, April, May (MAM), c) June, July, August (JJA) and observed 3-hourly periods with large hail events over the same period for b) MAM, d) JJA. 48

11 a) Climatological mean peak month at each gridpoint of observed large hail events 1979-2012, b) Climatological mean peak month at each gridpoint of the hail index 1979-2012. 49

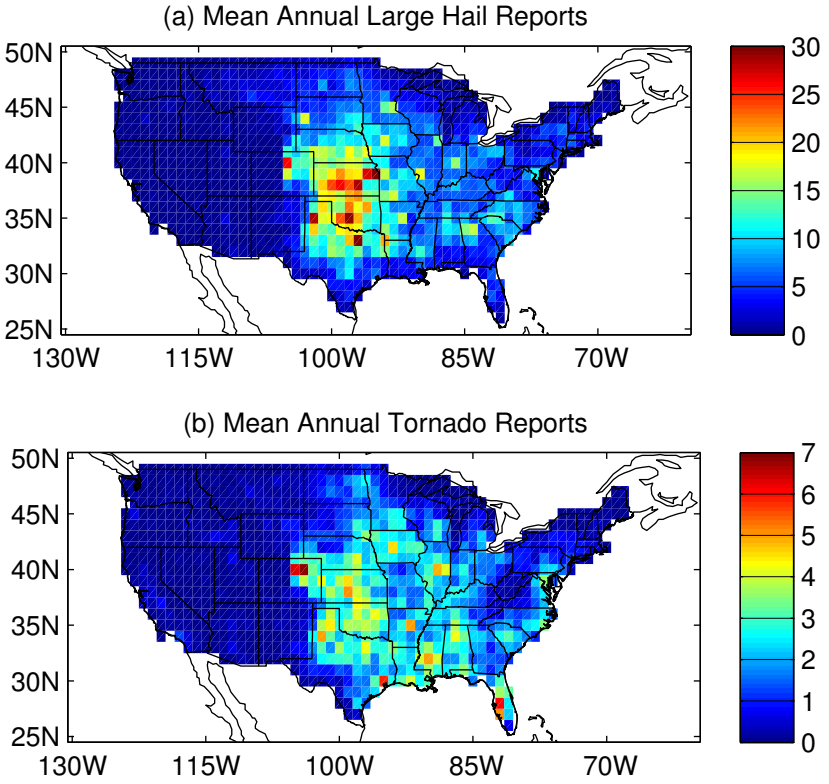

FIG. 1. a) Annual mean number of gridded ($1^\circ \times 1^\circ$) reports of hail equal to or greater than 1 inch 1979-2012, and b) Annual mean number of gridded ($1^\circ \times 1^\circ$) reports of tornadoes greater than F0 intensity for the same period.

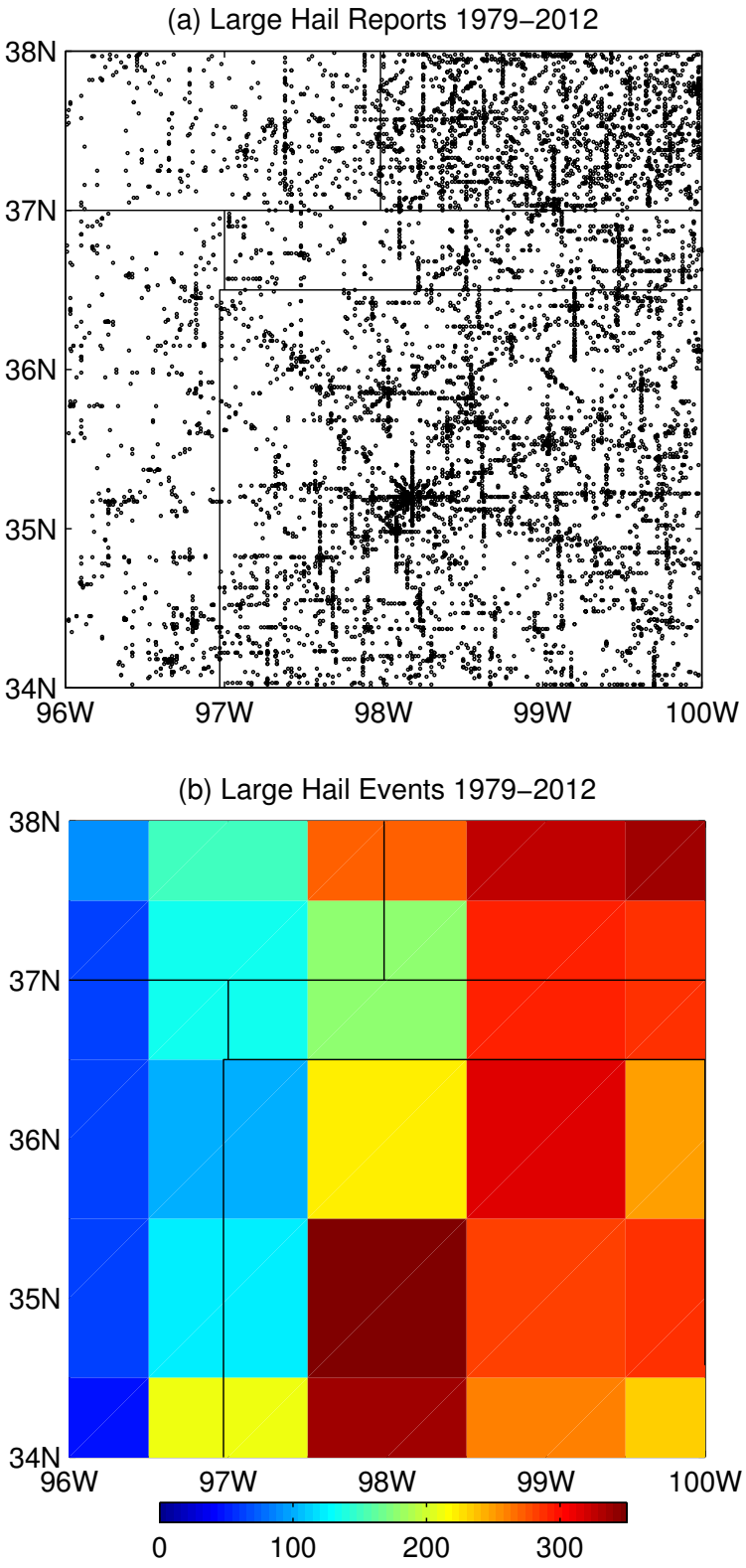

FIG. 2. a) Point reports of hail over the period 1979-2012 for the Texas panhandle and surrounding areas bounded by 34° to 38°N and 96° to 100°W from NCDC Hail observations, and b) Total number of gridded (1° × 1°) three hourly hail events (≥1 inch) for the same period and domain.

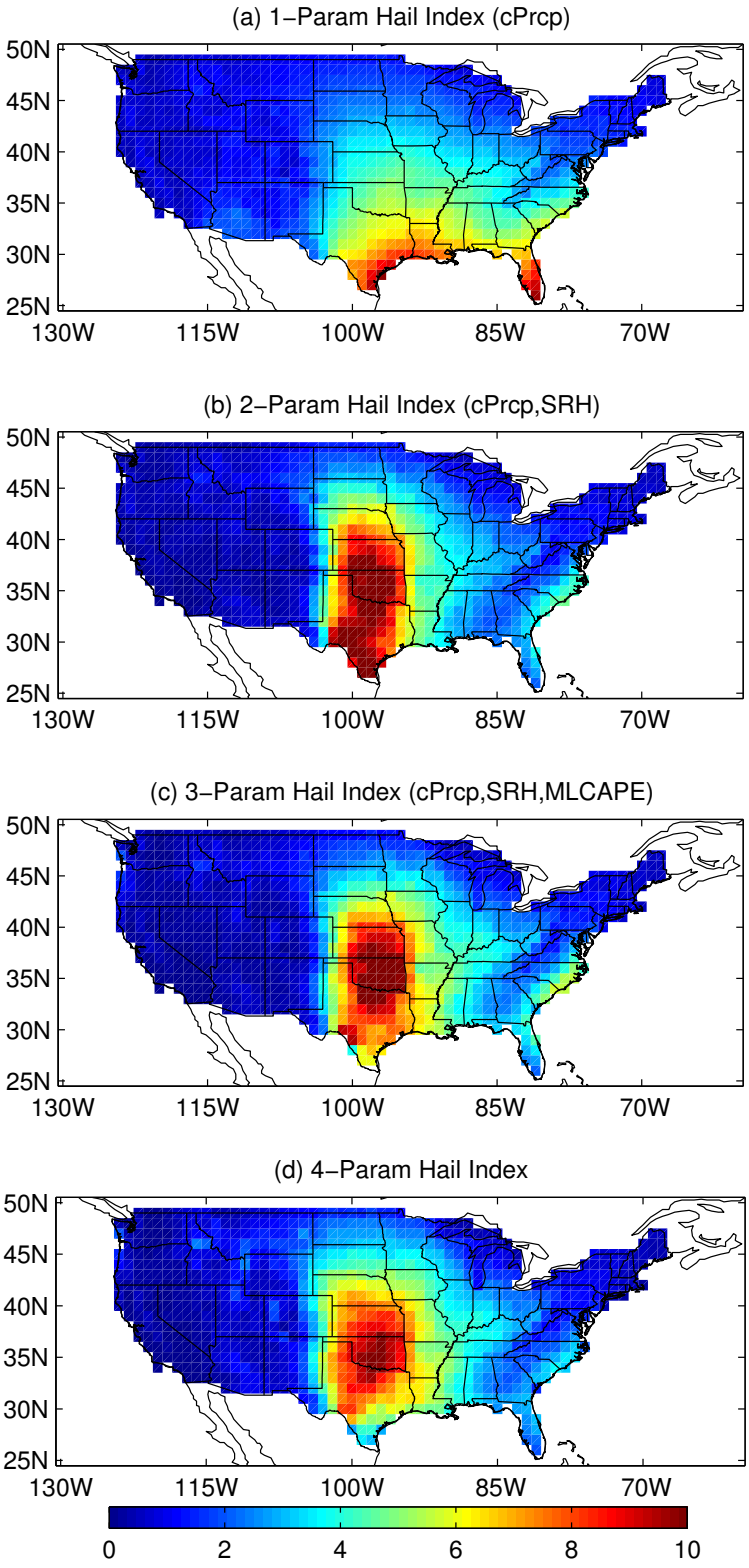

FIG. 3. Optimal deviance fitted Poisson regression indices for large hail events with increasing number environmental of parameters for the period 1979-2012. a) One parameter index (cPrcp), b) Two parameter index (cPrcp, SRH), c) Three parameter index (cPrcp, SRH, MLCAPE) and d) Four parameter index (cPrcp, SRH, MLCAPE, Qmean). Units are mean annual number of three hourly periods with hail events greater than one inch.

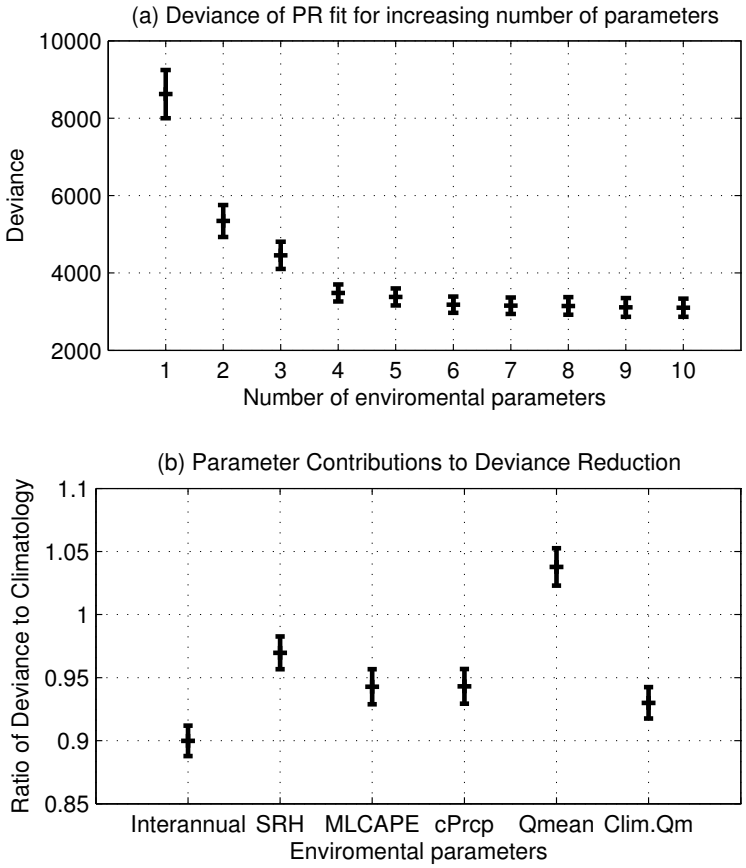

FIG. 4. a) Deviance of index fit for increasing number of environmental parameters. b) Contribution of the respective parameters to index deviance measured as a ratio of deviance using the interannually varying parameter to the climatological value.

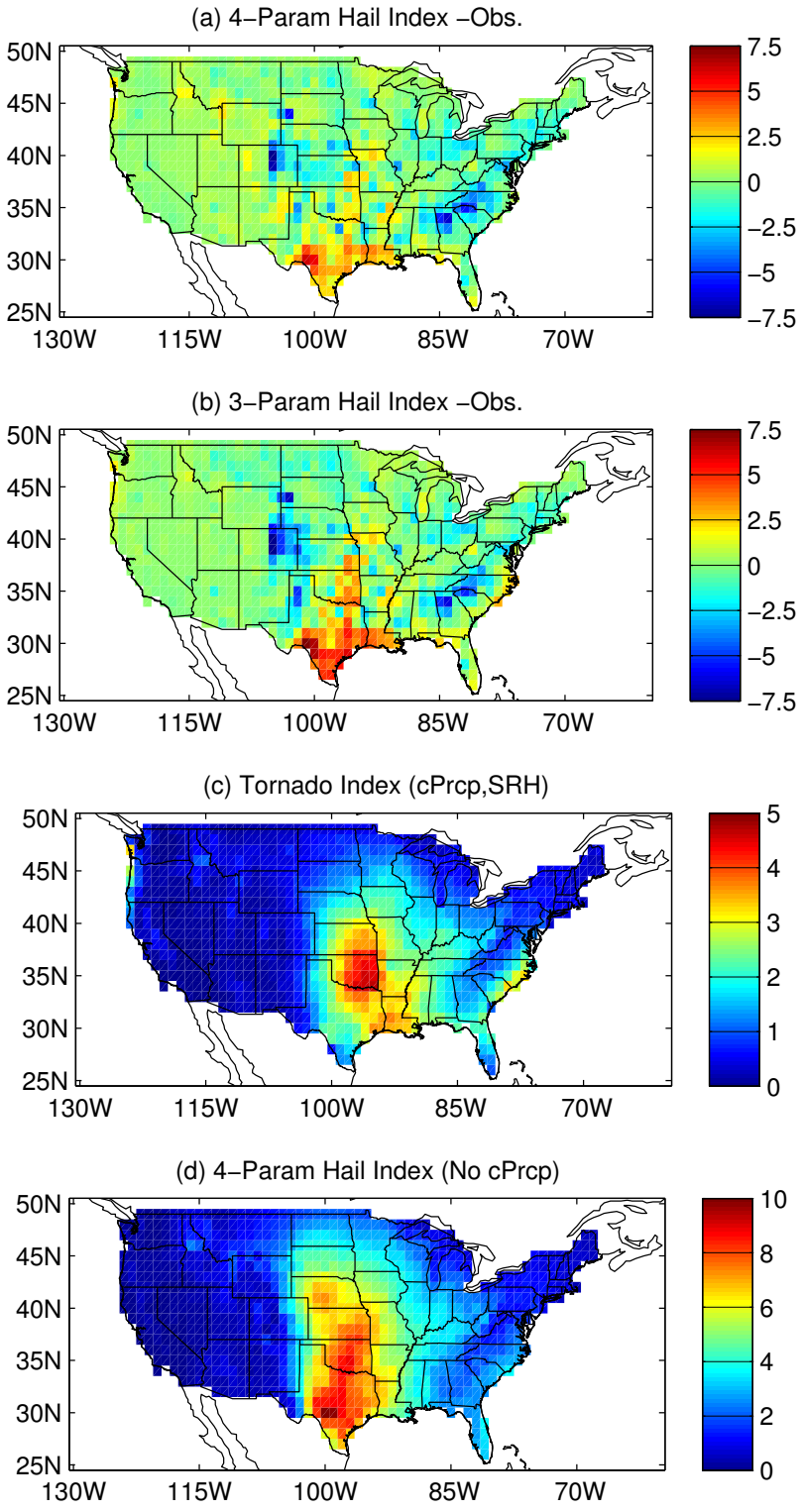

FIG. 5. a) Difference between the mean annual number of 3-hourly periods with hail events for the four parameter hail index and observed large hail events 1979-2012. b) As for a), except difference between mean annual number of the three parameter hail index events and observed large hail events. c) Mean annual number of three hourly periods with tornado events from the tornado index calculated using Eqn.2 for the same period. d) Mean annual number of large hail events of the 'next best' index without cPrcp included.

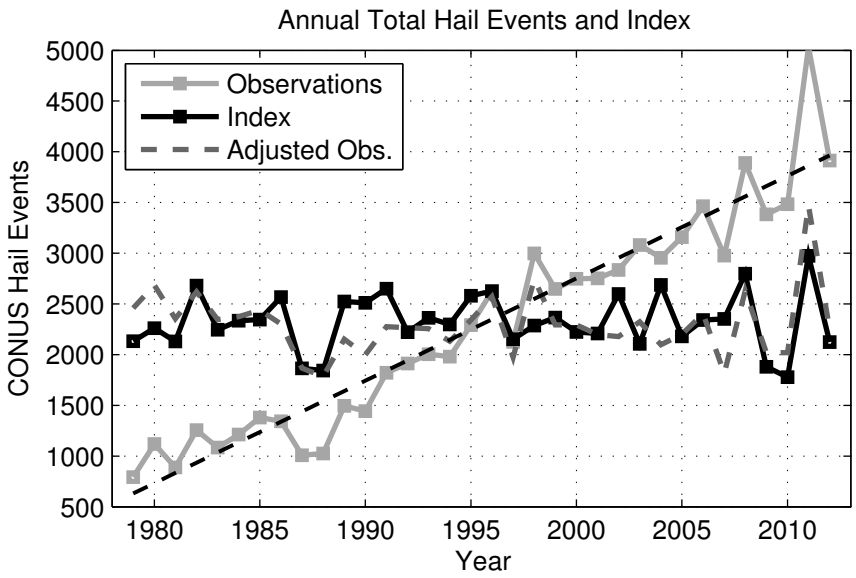

FIG. 6. Variability in annual CONUS total of hail events as compared to the index for the period 1979-2012. Grey line shows occurrence of large hail events over the respective regions, while the black line shows the annual frequency as simulated by the 4-parameter hail index. The adjusted observations (dashed grey) have been linearly detrended (trend shown in dashed black).

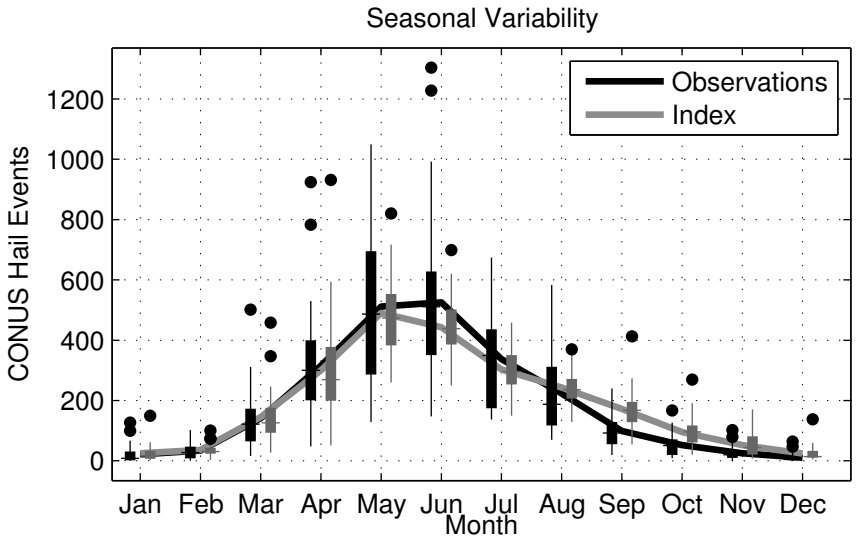

FIG. 7. Seasonal variability of the hail index for total monthly hail events over the CONUS as compared to observed hail events 1979-2012. Lines are mean index (grey) and observations (black) seasonal cycle, whiskers reflect 2.7σ of the distribution (99.3 percent). Dots show outlying years which are outside the 2.7σ range.

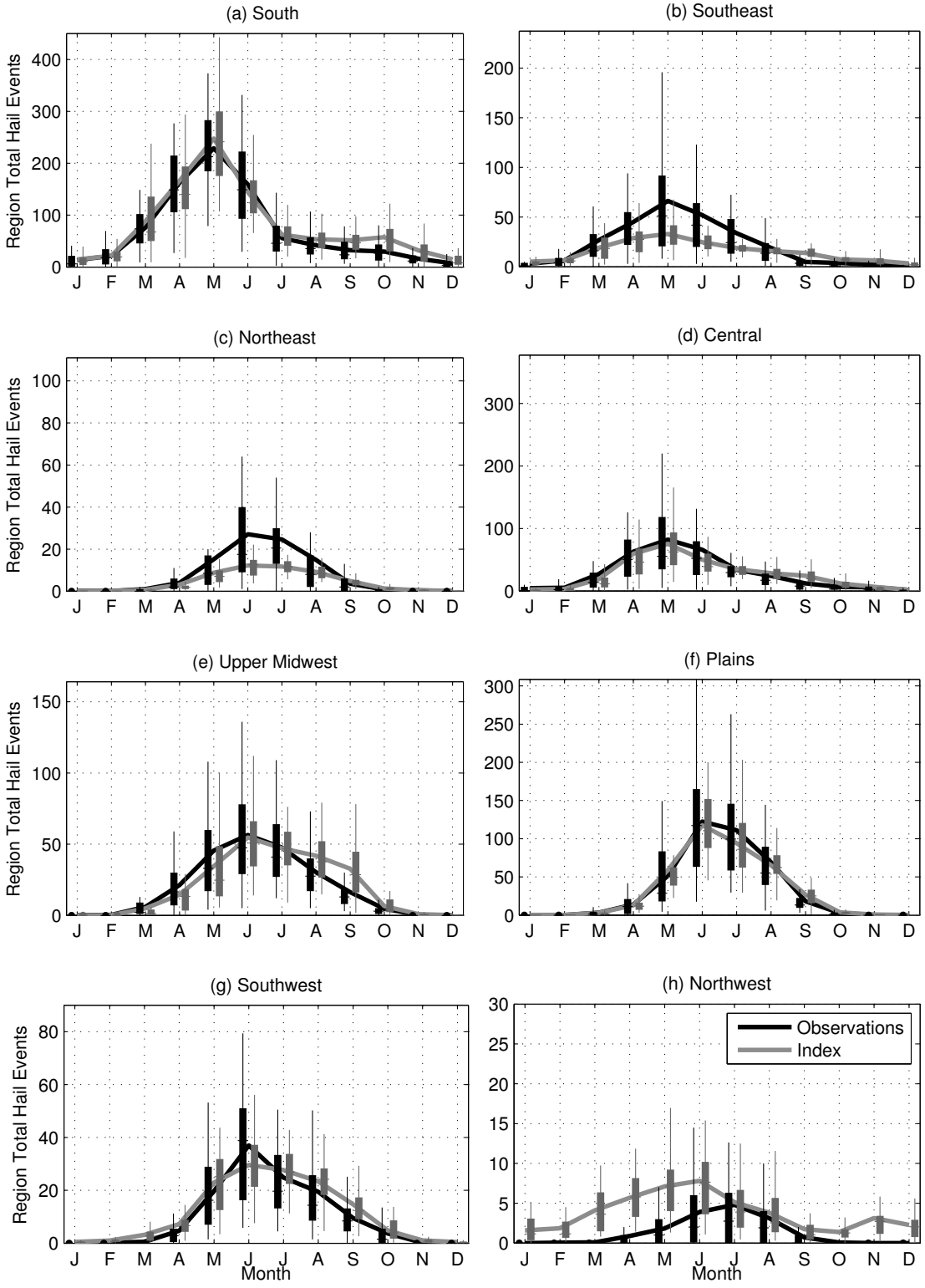

FIG. 8. As for Figure 7, except seasonal cycle of the index and observed hail events over the NOAA climate regions for a) South, b) Southeast, c) Northeast, d) Central, e) Upper Midwest, f) Plains, g) Southwest and h) Northwest. No outliers are shown.

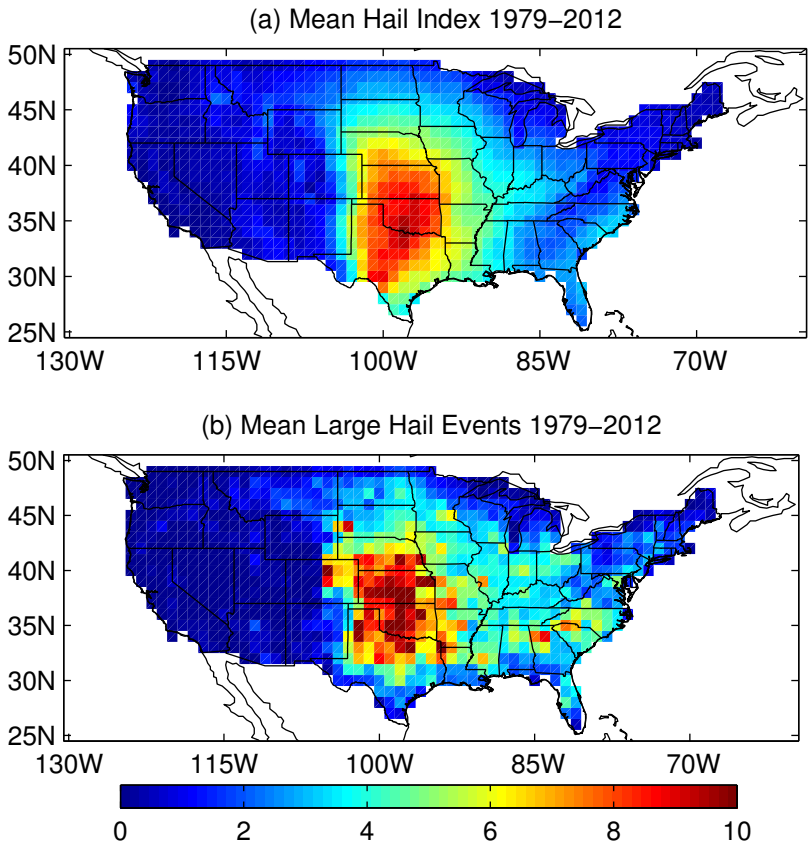

FIG. 9. a) Mean annual number of 3-hourly periods with large hail events as predicted by the four parameter index 1979-2012. b) As for a) except the mean annual occurrence of large hail events.

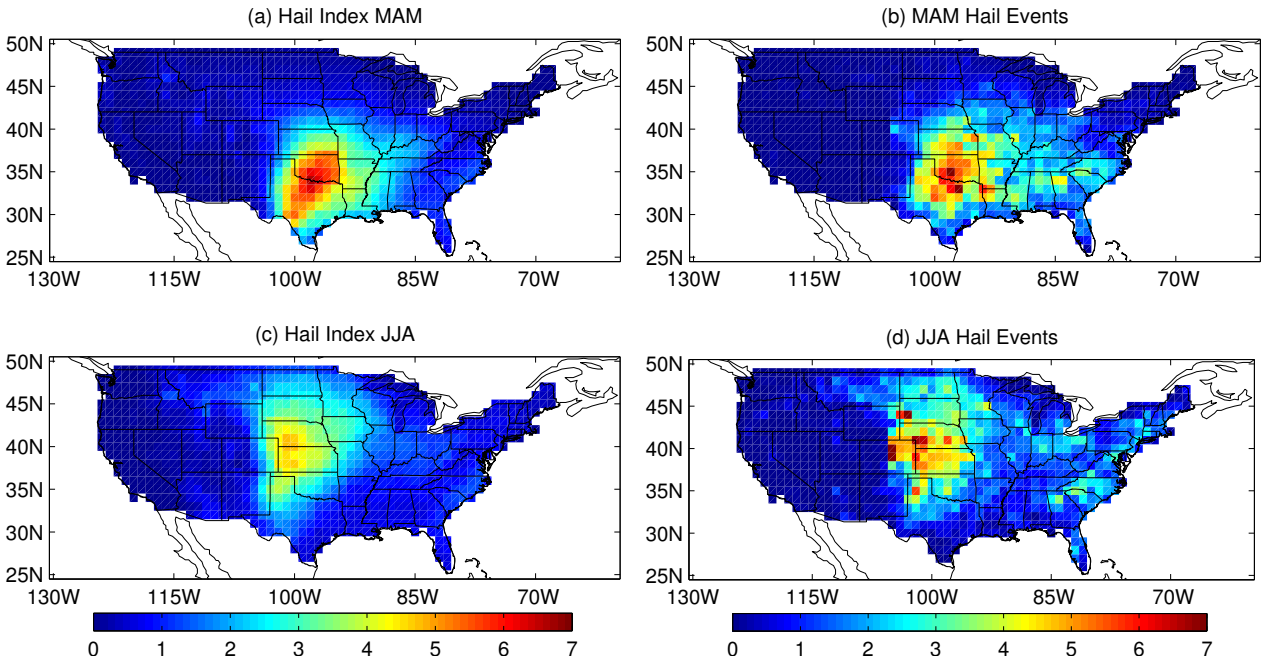

FIG. 10. Seasonal mean number of 3-hourly periods with large hail events from the four parameter index 1979-2012 for a) March, April, May (MAM), c) June, July, August (JJA) and observed 3-hourly periods with large hail events over the same period for b) MAM, d) JJA.

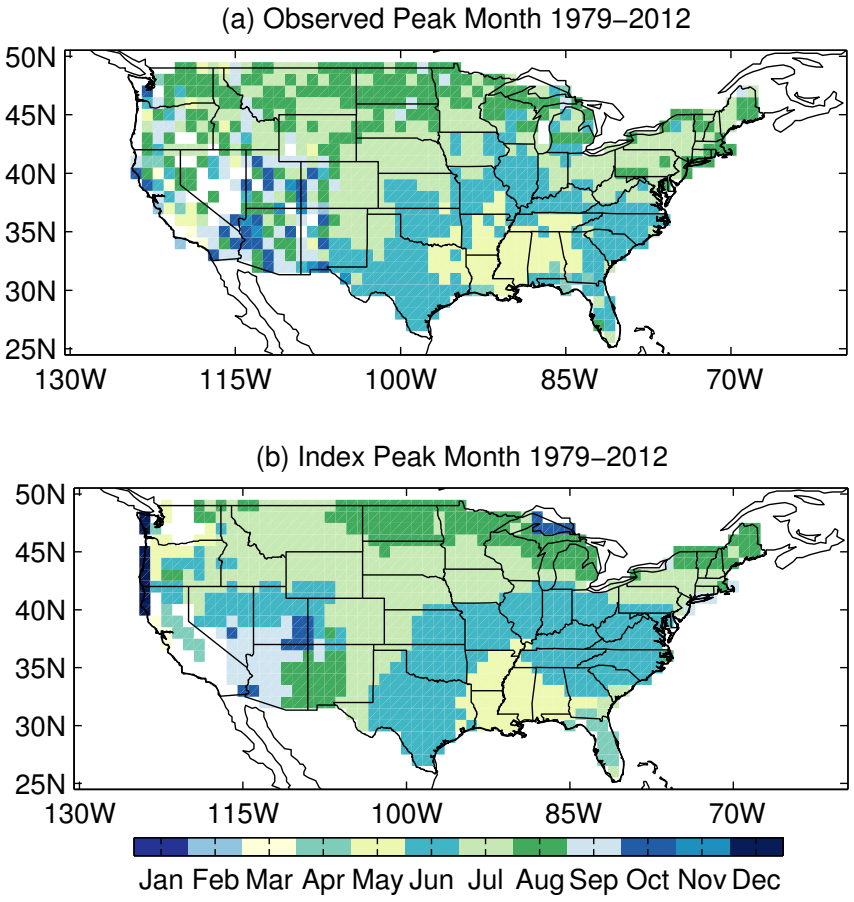

FIG. 11. a) Climatological mean peak month at each gridpoint of observed large hail events 1979-2012, b) Climatological mean peak month at each gridpoint of the hail index 1979-2012.